Computers, Materials & Continua CMC, vol.63, no.3, pp.1143-1157, 2020

Exact Solution of Non-Newtonian Blood Flow with Nanoparticles through Porous Arteries: A Comparative Study

Wafaa Alharbi[1], Abdulrahman Aljohani[1], Essam El-Zahar[2, 3, *] and Abdelhalim Ebaid[1]

Abstract: In this paper, the mathematical model describing the third-grade non-Newtonian blood flow suspended with nanoparticles through porous arteries is exactly solved. The present physical model was solved in the research literature via the optimal homotopy analysis method and the collocation method, where the obtained solution was compared with the numerical fourth-order Runge-Kutta solution. However, the present paper only introduces a new approach to obtain the exact solution of the concerned system and implements such exact solution as a reference to validate the published approximate solutions. Several remarks on the previously published results are observed and discussed in detail through tables and graphs. In view of the present calculations, the obtained results in the literature by Ghasemi et al. [Ghasemi, Hatami, Sarokolaie et al. (2015)] may need revisions. Furthermore, it is found that the obtained approximate results in the relevant literature agree with the current exact ones up to only two or three decimal places, at most. Hence, the present approach along with the obtained results reflexes the effectiveness and efficiency of our analysis when compared with the corresponding study in the literature. Moreover, the present results can be directly invested for similar future problems of the same constructions.

Keywords: Nanofluid, blood flow, porous artery, nanoparticle, exact solution.

1 Introduction

Presently, the study of nanofluid flow has gained the attention of many researchers [Metal and Gegel (1979); Karwe and Jaluria (1991); Chan (2009); Choi and Eastman (1995); Saidur, Leong and Mohammad (2011); Wang and Mujumdar (2007, 2008)] and is now of practical applications in engineering and medical sciences. Experiments showed that the thermal conductivity of a base-fluid can be enhanced by adding a small fraction of nanoparticles to such base-fluids [Xuan (2003); Chamkha, Rashad, El-Zahar et al. (2019); El-Zahar, Rashad and Seddek (2019)], and accordingly the heat transfer

[1] Department of Mathematics, Faculty of Science, University of Tabuk, Tabuk, 71491, Saudi Arabia.

[2] Department of Mathematics, College of Sciences and Humanities in Al-Kharj, Prince Sattam bin Abdulaziz University, Alkharj, 11942, Saudi Arabia.

[3] Department of Basic Engineering Science, Faculty of Engineering, Menofia University, Shebin El-Kom, 32511, Egypt.

[*] Corresponding Author: E. R. El-Zahar. Email: essam_zahar2006@yahoo.com; er.elzahar@psau.edu.sa.

Received: 20 October 2019; Accepted: 13 March 2020.

coefficient was improved for Newtonian nanofluids [Bachok, Ishak and Pop (2010); Aly and Ebaid (2016); Hamad (2011); Ebaid and Al Sharif (2015); Ebaid, Al Mutairi and Khaled (2014); Mabood, Khan and Rashidi (2017); Aly and Ebaid (2013)]. The progress in nanofluids including both types of Newtonian and non-Newtonian fluids are listed in the literature [Yadav, Bhargava and Agrawal (2013); Valinataj-Bahnemiri, Ramiar, Manavi et al. (2015); Yadav, Lee, Cho et al. (2016); Yadav (2017a, 2017b); Hady, Ibrahim, Abdel-Gaied et al. (2011); Hatami and Ganji (2013); Hady, Eid and Ahmed (2014); Eid (2016, 2017)].

Usually, the mathematical models describing such kind of problems are governed by systems of coupled linear/nonlinear ordinary and partial differential equations. To solve such systems, the researchers often resort to approximate numerical/analytical methods. However, the accuracy of the approximate methods should be validated in order to trust their results.

It has been shown in the literature Ebaid et al. [Ebaid (2014); Ebaid and Khaled (2014); Khaled, Ebaid and Almutairi (2014); Ebaid and Alatawi (2014); Almazmumy and Ebaid (2017); Ebaid, El-Zahar, Aljohani et al. (2019)] that some of the published approximate numerical/analytical solutions were not accurate enough. Moreover, the exact solution of any system is capable of detecting the accuracy of the approximated one by performing comparisons. As an example, Ghasemi et al. [Ghasemi, Hatami, Sarokolaie et al. (2015)] analyzed the system describing the blood flow suspended with nanoparticles through porous arteries using the Optimal Homotopy Analysis Method (OHAM) and the Collocation Method (CM) to obtain approximate analytical and numerical solutions, respectively.

Besides, they implemented the fourth-order Runge-Kutta method (4RKM) to validate their approximate analytical and numerical solutions where the exact solution is still unavailable. Therefore, the objective of this paper is to derive the exact solution of the system describing the blood flow suspended with nanoparticles through porous arteries under the influence of a magnetic field in the form:

$$\frac{d\mu}{dr}\frac{dv}{dr}+\mu\left(\frac{d^2v}{dr^2}+\frac{1}{r}\frac{dv}{dr}\right)+\Lambda\left(\frac{dv}{dr}\right)^2\left(3\frac{d^2v}{dr^2}+\frac{1}{r}\frac{dv}{dr}\right)=\left(P+M^2\right)v+c-Gr\theta-Br\phi \quad (1)$$

$$\alpha\frac{d^2\theta}{dr^2}+\frac{1}{r}\frac{d\theta}{dr}+Nb\frac{d\theta}{dr}\frac{d\phi}{dr}+\alpha_1 Nt\left(\frac{d\theta}{dr}\right)^2=0 \quad (2)$$

$$Nb\left(\frac{d^2\theta}{dr^2}+\frac{1}{r}\frac{d\theta}{dr}\right)+Nt\left(\frac{d^2\phi}{dr^2}+\frac{1}{r}\frac{d\phi}{dr}\right)=0 \quad (3)$$

subject to

$$v(1)=1,\ v(2)=0 \quad (4)$$

$$\theta(1)=1,\ \theta(2)=0 \quad (5)$$

$$\phi(1)=1,\ \phi(2)=0 \quad (6)$$

where $v(r)$, $\theta(r)$, and $\phi(r)$ are, respectively, the fluid velocity, the temperature, and the nanoparticles concentration. Also, μ is the viscosity of nanofluid, M is the magnetic parameter, P is the porosity parameter, c is the pressure gradient, Λ is the

third-grade parameter, Br is the Brownian diffusion constant, Gr is the Grashof number, Nb is Brownian motion parameter, Nt is the thermophoresis parameter, and α and α_1 are the material modules. The boundary conditions in Eqs. (4)-(6) describe the values of $v(r)$, $\theta(r)$, and $\phi(r)$ at the boundary of the inner and the outer coaxial cylinders. In terms of the temperature, the viscosity of the non-Newtonian nanofluid was considered as Vogel's model and given by:

$$\mu = \mu_0 e^{A\theta_0/(B+\theta)} \tag{7}$$

where A and B are constants and the subscript 0 denotes to the ambient condition. The paper is organized as follows. The exact solutions of Eqs. (2)-(3) with the boundary condition in Eqs. (5)-(6) will be obtained in Section 2. Section 3 is devoted to discuss two special cases. In Section 4, the numerical results of $v(r)$, $\theta(r)$, and $\phi(r)$ will be conducted for the purpose of comparisons with the corresponding results obtained by Ghasemi et al. [Ghasemi, Hatami, Sarokolaie et al. (2015)] literature. The obtained results are summarized and concluded in Section 5.

2 Exact solutions of $\theta(r)$ and $\phi(r)$

Let us begin this section with obtaining the explicit relation between $\theta(r)$ and $\phi(r)$. Integrating Eq. (3) twice with respect to r results in

$$Nb\theta + Nt\phi = a_1 \ln(r) + a_2 \tag{8}$$

where a_1 and a_2 are two constants to be determined. According to the boundary conditions in Eqs. (5)-(6), the constants a_1 and a_2 can be obtained as

$$a_1 = -\left(\frac{a_2}{\ln 2}\right), \quad a_2 = Nt + Nb \tag{9}$$

Eq. (8) implies that

$$\frac{d\phi}{dr} = \left(\frac{a_1}{Ntr}\right) - \frac{Nb}{Nt}\left(\frac{d\theta}{dr}\right) \tag{10}$$

Inserting Eq. (10) into Eq. (2), yields

$$\frac{d^2\theta}{dr^2} + \left(\frac{a_1 Nb + Nt}{\alpha Nt}\right)\frac{1}{r}\frac{d\theta}{dr} + \left(\frac{\alpha_1 (Nt)^2 - (Nb)^2}{\alpha Nt}\right)\left(\frac{d\theta}{dr}\right)^2 = 0 \tag{11}$$

Eq. (11) can be simplified by assuming that

$$\lambda = \frac{a_1 Nb + Nt}{\alpha Nt}, \ \sigma = \frac{\alpha_1 (Nt)^2 - (Nb)^2}{\alpha Nt}, \ \psi(r) = \frac{d\theta}{dr} \tag{12}$$

and therefore Eq. (11) reduces to

$$\frac{d\psi}{dr} + \left(\frac{\lambda}{r}\right)\psi(r) + \sigma\psi^2 = 0 \tag{13}$$

which is Bernoulli non-linear differential equation in ψ. In order to solve Eq. (13), the next assumption is useful

$$\chi(r)=\frac{1}{\psi(r)} \tag{14}$$

Accordingly, Eq. (13) reduces to the following linear differential equation in χ:

$$\frac{d\chi}{dr}-\left(\frac{\lambda}{r}\right)\chi(r)=\sigma \tag{15}$$

The solution of Eq. (15) can be obtained as

$$\chi(r)=\left(\frac{\sigma}{1-\lambda}\right)r+a_3 r^{\lambda},\ \text{such that}\quad \lambda\neq 1 \tag{16}$$

where a_3 is a constant. Therefore

$$\psi(r)=\frac{1}{\chi(r)}=\frac{1}{\left(\frac{\sigma}{1-\lambda}\right)r+a_3 r^{\lambda}} \tag{17}$$

Hence, the temperature $\theta(r)$ can be calculated from the last equation in Eq. (12) and given as

$$\theta(r)=\int\psi(r)dr=\int\frac{dr}{\left(\frac{\sigma}{1-\lambda}\right)r+a_3 r^{\lambda}}=\int\frac{r^{-\lambda}dr}{\left(\frac{\sigma}{1-\lambda}\right)r^{1-\lambda}+a_3} \tag{18}$$

and thus

$$\theta(r)=\frac{1}{\sigma}\ln\left[\left(\frac{\sigma}{1-\lambda}\right)r^{1-\lambda}+a_3\right]+a_4,\ \text{such that}\quad \sigma\neq 0 \tag{19}$$

where a_4 is an additional constant. Applying the conditions in Eq. (5) on Eq. (19), we then get the following system:

$$\frac{1}{\sigma}\ln\left[\left(\frac{\sigma}{1-\lambda}\right)+a_3\right]+a_4=1 \tag{20}$$

$$\frac{1}{\sigma}\ln\left[\left(\frac{\sigma}{1-\lambda}\right)2^{1-\sigma}+a_3\right]+a_4=0 \tag{21}$$

Solving this system, the constants a_3 and a_4 are determined in a simplest form as

$$a_3=\frac{\sigma}{1-\lambda}\left(\frac{(2)^{1-\lambda}e^{\sigma}-1}{1-e^{\sigma}}\right) \tag{22}$$

$$a_4=1-\frac{1}{\sigma}\ln\left[\left(\frac{\sigma}{1-\lambda}\right)\left(\frac{(2)^{1-\lambda}-1}{e^{-\sigma}-1}\right)\right] \tag{23}$$

Inserting Eqs. (22) and (23) into Eq. (19) and simplifying, we obtain $\theta(r)$ in its final form as

$$\theta(r)=1+\frac{1}{\sigma}\ln\left[\frac{\left(1-e^{\sigma}\right)r^{1-\lambda}+(2)^{1-\lambda}e^{\sigma}-1}{\left((2)^{1-\lambda}-1\right)e^{\sigma}}\right],\ \sigma\neq 0,\ \lambda\neq 1. \tag{24}$$

We have from Eq. (8) that

$$\phi(r)=\left(\frac{a_1}{Nt}\right)\ln(r)+\frac{a_2}{Nt}-\left(\frac{Nb}{Nt}\right)\theta(r) \tag{25}$$

Using Eqs. (9) and (24) in Eq. (25) we obtain the following final form of $\phi(r)$:

$$\phi(r)=1-\left(\frac{Nb}{Nt}+1\right)\left(\frac{\ln(r)}{\ln(2)}\right)-\left(\frac{Nb}{\sigma Nt}\right)\ln\left[\frac{\left(1-e^{\sigma}\right)r^{1-\lambda}+(2)^{1-\lambda}e^{\sigma}-1}{\left((2)^{1-\lambda}-1\right)e^{\sigma}}\right] \tag{26}$$

3 Special cases

3.1 At $\sigma\to 0$

In this case, we have from Eq. (12) that

$$\alpha_1=\left(\frac{Nb}{Nt}\right)^2 \tag{27}$$

Here, the exact solutions of $\theta(r)$ and $\phi(r)$ can be obtained by calculating the limits of Eqs. (24) and (26), respectively, as $\sigma\to 0$, and given by

$$\theta(r)=\frac{(2)^{1-\lambda}-r^{1-\lambda}}{(2)^{1-\lambda}-1} \tag{28}$$

and

$$\phi(r)=1-\left(\frac{Nb}{Nt}+1\right)\left(\frac{\ln(r)}{\ln(2)}\right)+\left(\frac{Nb}{Nt}\right)\left(\frac{1-r^{1-\lambda}}{1-(2)^{1-\lambda}}\right) \tag{29}$$

3.2 At $\lambda\to 1$

As $\lambda\to 1$, we have from Eqs. (9) and (12) that

$$a_1=-\left(\frac{Nb+Nt}{\ln(2)}\right),\ a_1=(\alpha-1)\left(\frac{Nt}{Nb}\right) \tag{30}$$

The relations in Eq. (30) are compacted to give the following restriction on α, Nb, and Nt:

$$(\alpha-1)\left(\frac{Nt}{Nb}\right)+\left(\frac{Nb+Nt}{\ln(2)}\right)=0 \tag{31}$$

In this case, Eq. (13) becomes

$$\frac{d\chi}{dr}-\left(\frac{1}{r}\right)\chi(r)=\sigma \tag{32}$$

The solution of Eq. (32) can be obtained as

$$\chi(r)=\sigma r\ln(r)+a_5 r \tag{33}$$

where a_5 is a constant. Therefore

$$\psi(r)=\frac{1}{\chi(r)}=\frac{1}{\sigma r\ln(r)+a_5 r} \tag{34}$$

Hence, the temperature $\theta(r)$ can be calculated from the last equation in Eq. (12) and given as

$$\theta(r)=\int\psi(r)dr=\int\frac{dr}{\sigma r\ln(r)+a_5 r}=\int\frac{r^{-1}dr}{\sigma\ln(r)+a_5} \tag{35}$$

and thus

$$\theta(r)=\frac{1}{\sigma}\ln\left(\sigma\ln(r)+a_5\right)+a_6 \tag{36}$$

where a_6 is an additional constant. Applying the conditions in Eq. (5) on Eq. (36), we then get the following system:

$$\frac{1}{\sigma}\ln(a_5)+a_6=1 \tag{37}$$

$$\frac{1}{\sigma}\ln\left(\sigma\ln(2)+a_5\right)+a_6=0 \tag{38}$$

Solving this system, the constants a_5 and a_6 are determined in a simplest form as

$$a_5=\frac{\sigma\ln(2)}{e^{-\sigma}-1} \tag{39}$$

$$a_6=1-\frac{1}{\sigma}\ln\left(\frac{\sigma\ln(2)}{e^{-\sigma}-1}\right) \tag{40}$$

Inserting Eqs. (39) and (40) into Eq. (36) and simplifying, we obtain $\theta(r)$ in its final form as

$$\theta(r)=1+\frac{1}{\sigma}\ln\left[\left(e^{-\sigma}-1\right)\left(\frac{\ln(r)}{\ln(2)}\right)+1\right],\ \sigma\neq 0 \tag{41}$$

Implementing Eq. (8) and Eq. (41), we obtain $\phi(r)$ as

$$\phi(r)=1+\left(\frac{\alpha-1}{Nb}\right)\ln(r)-\left(\frac{Nb}{\sigma Nt}\right)\ln\left[\left(e^{-\sigma}-1\right)\left(\frac{\ln(r)}{\ln(2)}\right)+1\right],Nb\neq 0,Nt\neq 0 \tag{42}$$

where the relation in Eq. (31) is also implemented to obtain the last equation.

4 Comparisons with published results

In their research paper, the authors Ghasemi et al. [Ghasemi, Hatami, Sarokolaie et al. (2015)] obtained the approximate analytical solutions for the present problem via the OHAM and the CM. They have implemented 4RKM as a reference method to stand on the accuracy of their approximate solutions. However, it has been shown in the previous section that the exact solutions for $\theta(r)$ and $\phi(r)$ were successfully obtained, hence, such exact solutions are to be invested here to estimate the accuracy of the published results. In addition, our numerical calculations for $v(r)$ is based on substituting the exact forms for $\theta(r)$ and $\phi(r)$ into (1) and then solving the resulting equation via MATHEMATICA. When all constants are assumed to be units, $c=-1$, and $Nt=Nb=2$, the obtained approximate $\theta(r)$, $\phi(r)$, and $v(r)$ via the CM by Ghasemi et al. [Ghasemi, Hatami, Sarokolaie et al. (2015)] were expressed as:

$$\theta(r)=(2-r)+2.400839451(2-r)(1-r)-1.044530104(4-r^2)(1-r) \tag{43}$$

$$\phi(r)=(2-r)-0.6971357470(2-r)(1-r)+0.7482338079(4-r^2)(1-r) \tag{44}$$

$$v(r)=(2-r)+0.6618326283(2-r)(1-r)-0.1908202534(4-r^2)(1-r) \tag{45}$$

The CM approximations in Eqs. (43)-(45) and the exact solutions are depicted in Fig. 1, Figs. 2 and 3. It is observed from these figures that the CM approximation in Eq. (45) for $v(r)$ is too close to the corresponding exact solution, while the CM approximations in Eqs. (43)-(44) for $\theta(r)$ and $\phi(r)$, respectively, are shifted by some amount from the corresponding exact solutions. In addition, the obtained errors by the CM are displayed in Fig. 4 which demonstrates that $Error|_{v(r)} < Error|_{\theta(r)} < Error|_{\phi(r)}$. Moreover, Fig. 4 indicates that the maximum errors of the CM for $\theta(r)$, $\phi(r)$, and $v(r)$ are 0.015, 0.020, and 0.007, respectively. For that, the CM approximation of $v(r)$ is of higher accuracy than the approximations of $\theta(r)$ and $\phi(r)$ when $Nt=Nb=2$.

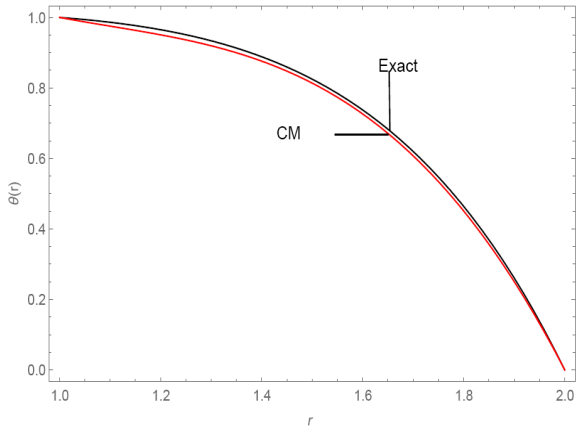

Figure 1: Exact and CM solutions for $\theta(r)$ at $Nt=Nb=2$

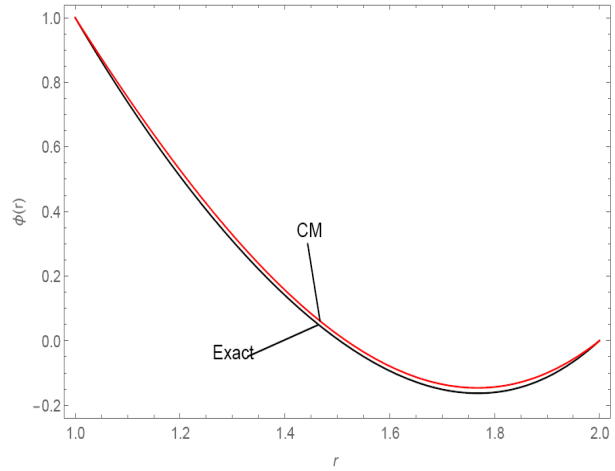

Figure 2: Exact and CM solutions for $\phi(r)$ at $Nt = Nb = 2$

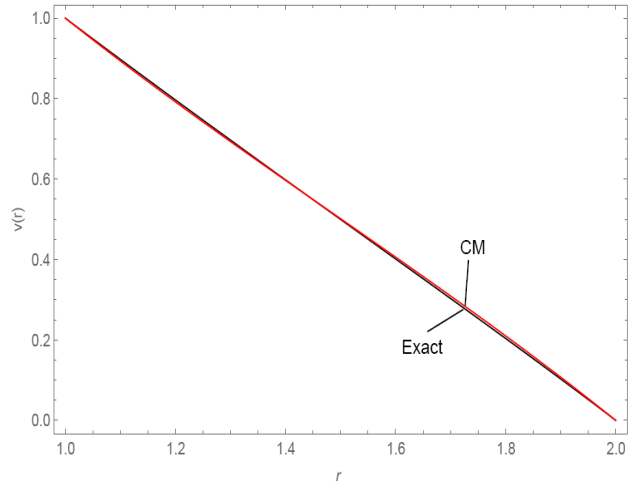

Figure 3: Exact and CM solutions for $v(r)$ at $Nt = Nb = 2$

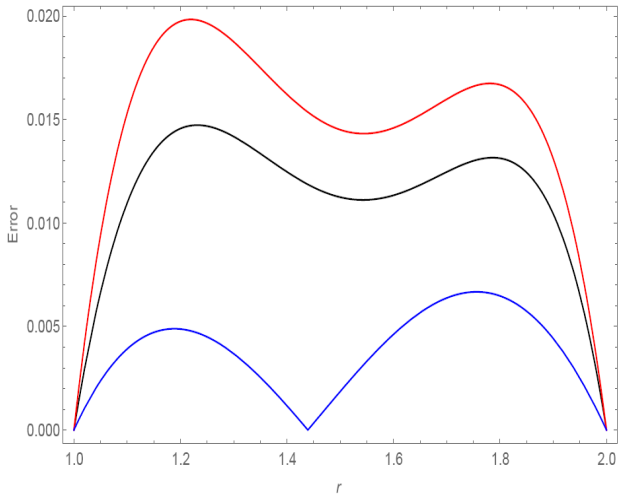

Figure 4: Errors of CM for $\theta(r)$ (Black), $\phi(r)$ (Red) and $v(r)$ (Blue)

Numerically, the values of $\theta(r)$, $\phi(r)$, and $v(r)$ by the CM using Eqs. (43)-(45) and the OHAM by Ghasemi et al. [Ghasemi, Hatami, Sarokolaie et al. (2015)] are listed in Tabs. 1-3, respectively, along with the obtained corresponding errors. The results of Tabs. 1-3 reveal that the CM and the OHAM are of similar accuracy when $Nt = Nb = 2$, but the situation may be changed at another set of values of the parameter Nt and Nb as discussed below. The numerical results listed in Tabs. 4-6 show that the CM is more accurate than the OHAM when $Nt = Nb = 1$ and this conclusion can also be observed from Tabs. 7-9 when $Nt = Nb = 0.5$.

As a final remark, we have noticed that the calculations reported by the authors Ghasemi et al. [Ghasemi, Hatami, Sarokolaie et al. (2015)] (Tabs. 1 and 2) for the values of $\theta(r)$ and $\phi(r)$ in the domain $r \in (1,2)$ were introduced in an incorrect manner. For example, when using Eqs. (43)-(44) to calculate $\theta(r)$ and $\phi(r)$ we can easily detect that the resulting values are completely different than those published ones, listed in (Tab. 1 and 2). In addition, we noticed that the previously obtained approximate results via the CM and OHAM agree with the current exact ones up to only two or three decimal places, at most. Consequently, the above discussion confirms the advantage of our approach over the previous published study.

Table 1: Comparison of the present exact solution with CM and OHAM in predicting $\theta(r)$ values at $Nt = Nb = 2$

r	Exact (Present)	CM	OHAM	Error	
				CM	OHAM
1.0	1.000000	1.000000	1.000000	0.000000	0.000000
1.1	0.986319	0.975348	0.975348	0.010971	0.010971
1.2	0.965227	0.950665	0.950665	0.014562	0.014562
1.3	0.933858	0.919683	0.919683	0.014175	0.014175
1.4	0.888604	0.876135	0.876135	0.012469	0.012469
1.5	0.825000	0.813754	0.813754	0.011246	0.011246
1.6	0.737609	0.726273	0.726273	0.011336	0.011336
1.7	0.619889	0.607424	0.607423	0.012466	0.012466
1.8	0.464068	0.450940	0.450940	0.013128	0.013128
1.9	0.260995	0.250555	0.250555	0.010440	0.010440
2.0	0.000000	0.000000	0.000000	0.000000	0.000000

Table 2: Comparison of the present exact solution with CM and OHAM in predicting $\phi(r)$ values at $Nt = Nb = 2$

r	Exact (Present)	CM	OHAM	Error	
				CM	OHAM
1.0	1.000000	1.000000	1.000000	0.000000	0.000000
1.1	0.738674	0.753985	0.753985	0.015311	0.015311
1.2	0.508704	0.528446	0.528446	0.019742	0.019742
1.3	0.309119	0.327872	0.327872	0.018754	0.018753
1.4	0.140543	0.156754	0.156754	0.016211	0.016211
1.5	0.005075	0.019579	0.019579	0.014504	0.014504
1.6	-0.093752	-0.079161	-0.079161	0.014591	0.014591
1.7	-0.150959	-0.134979	-0.134979	0.015980	0.015980
1.8	-0.160062	-0.143384	-0.143384	0.016677	0.016678
1.9	-0.112993	-0.099888	-0.099888	0.013106	0.013105
2.0	0.000000	0.000000	0.000000	0.000000	0.000000

Table 3: Comparison of the present exact solution with CM and OHAM in predicting $v(r)$ values at $Nt = Nb = 2$

r	Exact (Present)	CM	OHAM	Error	
				CM	OHAM
1.0	1.000000	1.000000	1.000000	0.000000	0.000000
1.1	0.897589	0.893674	0.88704	0.003915	0.003915
1.2	0.796681	0.791807	0.77952	0.004875	0.004874
1.3	0.696941	0.693254	0.67648	0.003687	0.003687
1.4	0.598041	0.596869	0.57696	0.001172	0.001172
1.5	0.499650	0.501510	0.48000	0.001860	0.001860
1.6	0.401408	0.406029	0.38464	0.004621	0.004621
1.7	0.302906	0.309282	0.28992	0.006377	0.006376
1.8	0.203649	0.210125	0.19488	0.006476	0.006476
1.9	0.102991	0.107413	0.09856	0.004423	0.004422
2.0	0.000000	0.000000	0.000000	0.000000	0.000000

Table 4: Comparison of the present exact solution with CM and OHAM in predicting $\theta(r)$ values at $Nt = Nb = 1$

r	Exact (Present)	CM	OHAM	Error	
				CM	OHAM
1.0	1.000000	1.000000	1.000000	0.000000	0.000000
1.1	0.950456	0.950804	0.943005	0.000348	0.007451
1.2	0.891648	0.892162	0.877897	0.000514	0.013751
1.3	0.822834	0.823382	0.804134	0.000548	0.018700
1.4	0.743280	0.743773	0.721176	0.000493	0.022104
1.5	0.652257	0.652645	0.628480	0.000388	0.023777
1.6	0.549042	0.549304	0.525506	0.000262	0.023536
1.7	0.432918	0.433061	0.411713	0.000143	0.021205
1.8	0.303174	0.303223	0.286558	0.000049	0.016616
1.9	0.159102	0.159100	0.149501	0.000002	0.009601
2.0	0.000000	0.000000	0.000000	0.000000	0.000000

Table 5: Comparison of the present exact solution with CM and OHAM in predicting $\phi(r)$ values at $Nt = Nb = 1$

r	Exact (Present)	CM	OHAM	Error	
				CM	OHAM
1.0	1.000000	1.000000	1.000000	0.000000	0.000000
1.1	0.774537	0.778529	0.786719	0.003992	0.012182
1.2	0.582283	0.586949	0.601669	0.004666	0.019386
1.3	0.420142	0.424174	0.443704	0.004032	0.023562
1.4	0.285866	0.156754	0.311676	0.129112	0.025810
1.5	0.177818	0.180689	0.204439	0.002871	0.026621
1.6	0.094815	0.097807	0.120847	0.002992	0.026032
1.7	0.036013	0.039384	0.059754	0.003371	0.023741
1.8	0.000832	0.004332	0.020012	0.003500	0.019180
1.9	-0.011101	-0.008430	0.000476	0.002671	0.011577
2.0	0.000000	0.000000	0.000000	0.000000	0.000000

Table 6: Comparison of the present exact solution with CM and OHAM in predicting $v(r)$ values at $Nt = Nb = 1$

r	Exact (Present)	CM	OHAM	Error	
				CM	OHAM
1.0	1.000000	1.000000	1.000000	0.000000	0.000000
1.1	0.898404	0.884070	0.876846	0.075959	0.021558
1.2	0.798095	0.771594	0.758641	0.026501	0.039454
1.3	0.698725	0.662605	0.645457	0.036120	0.053268
1.4	0.599962	0.557135	0.537369	0.042827	0.062593
1.5	0.501474	0.455216	0.434451	0.046258	0.067023
1.6	0.402917	0.356880	0.336778	0.046037	0.066139
1.7	0.303922	0.262158	0.244421	0.041764	0.059501
1.8	0.204087	0.171083	0.157457	0.033004	0.04663
1.9	0.102956	0.083686	0.075959	0.019270	0.026997
2.0	0.000000	0.000000	0.000000	0.000000	0.000000

Table 7: Comparison of the present exact solution with CM and OHAM in predicting $\theta(r)$ values at $Nt = Nb = 0.5$

r	Exact (Present)	CM	OHAM	Error	
				CM	OHAM
1.0	1.000000	1.000000	1.000000	0.000000	0.000000
1.1	0.914213	0.907045	0.907045	0.007168	0.007168
1.2	0.824900	0.824985	0.812185	0.000085	0.012715
1.3	0.732227	0.732347	0.715547	0.000120	0.016680
1.4	0.636341	0.636458	0.617258	0.000117	0.019083
1.5	0.537373	0.537446	0.517446	0.000073	0.019927
1.6	0.435439	0.435438	0.416238	0.000001	0.019201
1.7	0.330643	0.330562	0.313762	0.000081	0.016881
1.8	0.223081	0.222946	0.210146	0.000135	0.012935
1.9	0.112841	0.112716	0.105516	0.000125	0.007325
2.0	0.000000	0.000000	0.000000	0.000000	0.000000

Table 8: Comparison of the present exact solution with CM and OHAM in predicting $\phi(r)$ values at $Nt = Nb = 0.5$

r	Exact (Present)	CM	OHAM	Error	
				CM	OHAM
1.0	1.000000	1.000000	1.000000	0.000000	0.000000
1.1	0.810780	0.815088	0.821989	0.004308	0.011209
1.2	0.649031	0.654126	0.666394	0.005095	0.017363
1.3	0.510750	0.515209	0.531310	0.004459	0.020560
1.4	0.392805	0.396431	0.414833	0.003626	0.022028
1.5	0.292702	0.295887	0.315056	0.003185	0.022354
1.6	0.208418	0.211673	0.230075	0.003255	0.021657
1.7	0.138287	0.141882	0.157984	0.003595	0.019697
1.8	0.080925	0.084610	0.096878	0.003685	0.015953
1.9	0.035161	0.037951	0.044852	0.00279	0.009691
2.0	0.000000	0.000000	0.000000	0.000000	0.000000

Table 9: Comparison of the present exact solution with CM and OHAM in predicting $v(r)$ values at $Nt = Nb = 0.5$

r	Exact (Present)	CM	OHAM	Error	
				CM	OHAM
1.0	1.000000	1.000000	1.000000	0.000000	0.000000
1.1	0.898944	0.882342	0.874947	0.016602	0.023997
1.2	0.798978	0.768684	0.755572	0.030294	0.043406
1.3	0.699768	0.658997	0.641834	0.040771	0.057934
1.4	0.601000	0.553252	0.533690	0.047748	0.067310
1.5	0.502366	0.451422	0.431100	0.050944	0.071266
1.6	0.403554	0.353479	0.334022	0.050075	0.069532
1.7	0.304249	0.259393	0.242415	0.044856	0.061834
1.8	0.204121	0.169163	0.156236	0.034958	0.047885
1.9	0.102826	0.082682	0.075445	0.020144	0.027381
2.0	0.000000	0.000000	0.000000	0.000000	0.000000

5 Conclusion

The exact solution of the system describing the third grade non-Newtonian blood flow suspended with nanoparticles through porous arteries was provided. Moreover, the exact solutions for two useful special cases were obtained. The developed exact solutions, for the phenomenon at hand, were compared with the published approximate results in the research literature using the OHAM and the CM. The comparisons revealed that, in most cases, the CM was of higher accuracy than the OHAM. Furthermore, the CM and OHAM results obtained by Ghasemi et al. [Ghasemi, Hatami, Sarokolaie et al. (2015)] agree with the current exact solutions up to only two decimal places in most of the investigated cases. The developed exact approach may be trustily recommended to study similar physical models in future.

Funding Statement: The authors would like to thank the referees for their valuable comments and suggestions which helped to improve the manuscript. Moreover, the third author acknowledges that this publication was supported by the Deanship of Scientific Research at Prince Sattam bin Abdulaziz University.

Conflicts of Interest: The authors declare no conflict of interest.

References

Almazmumy, M.; Ebaid, A. (2017): Exact analysis of the flow and heat transfer of the SA-TiO2 non-Newtonian nanofluid between two coaxial cylinders through a porous medium. *Zeitschrift für Naturforschung A*, vol. 72, no. 9, pp. 855-862.

Aly, E. H.; Ebaid, A. (2013): Exact analytical solution for suction and injection flow with thermal enhancement of five nanofluids over an isothermal stretching sheet with effect of the slip model: a comparative study. *Abstract and Applied Analysis*, vol. 2013, pp. 1-14, http://dx.doi.org/10.1155/2013/721578.

Aly, E. H.; Ebaid, A. (2016): New exact solutions for boundary-layer flow of a nanofluid past a stretching sheet. *Journal of Computational and Theoretical Nanoscience*, vol. 10, no. 1, pp. 2591-2594.

Bachok, N.; Ishak, A.; Pop, I. (2010): Boundary-layer flow of nanofluids over a moving surface in a flowing fluid. *International Journal of Thermal Sciences*, vol. 49, no. 9, pp. 1663-1668.

Chamkha, A. J.; Rashad, A. M.; El-Zahar, E. R.; El-Mky, H. A. (2019): Analytical and numerical investigation of Fe_3O_4-water nanofluid flow over a moveable plane in a parallel stream with high suction. *Energies*, vol. 12, no. 1, pp. 1-18.

Chan, C. W. C. (2009): Bio-Applications of Nanoparticles, *Springer Science & Business Media*, New York.

Choi, S. U.; Eastman, J. A. (1995): Enhancing thermal conductivity of fluids with nanoparticles. *Developments and Applications of Non-Newtonian Flows,* vol. 66, pp. 99-105. ASME, New York.

Ebaid, A. (2014): Remarks on the homotopy perturbation method for the peristaltic flow of Jeffrey fluid with nanoparticles in an asymmetric channel. *Computers and Mathematics with Applications*, vol. 68, no. 2014, pp. 77-85.

Ebaid, A.; Al Mutairi, F.; Khaled, S. M. (2014): Effect of velocity slip boundary condition on the flow and heat transfer of Cu-Water and TiO 2-Water nanofluids in the presence of a magnetic field. *Advances in Mathematical Physics*, vol. 2014, pp. 1-9, http://dx.doi.org/10.1155/2014/538950.

Ebaid, A.; Al Sharif, M. A. (2015): Application of Laplace transform for the exact effect of a magnetic field on heat transfer of carbon nanotubes-suspended nanofluids. *Zeitschrift für Naturforschung A*, vol. 70, no. 6, pp. 471-475.

Ebaid, A.; El-Zahar, E. R.; Aljohani, A. F.; Salah, B.; Krid, M. et al. (2019): Exact solutions of the generalized nonlinear Fokas-Lennells equation. *Results in Physics*, vol. 14, no. 2019.

Ebaid, A.; Khaled, S. M. (2014): An exact solution for a boundary value problem with application in fluid mechanics and comparison with the regular perturbation solution. *Abstract and Applied Analysis*, vol. 2014, pp. 1-7.

Eid, M. R. (2016): Chemical reaction effect on MHD boundary-layer flow of two-phase nanofluid model over an exponentially stretching sheet with a heat generation. *Journal of Molecular Liquids*, vol. 220, no. 2016, pp. 718-725.

Eid, M. R. (2017): Time-dependent flow of water-NPs over a stretching sheet in a saturated porous medium in the stagnation-point region in the presence of chemical reaction. *Journal of Nanofluids*, vol. 6, no. 3, pp. 550-557.

EL-Zahar, E. R.; Rashad.; A. M.; Seddek, L. F. (2019). The impact of sinusoidal surface temperature on the natural convective flow of a ferrofluid along a vertical plate. *Mathematics*, vol. 7, no. 11, pp. 1014. https://doi.org/10.3390/math7111014.

Ghasemi, S. E.; Hatami, M.; Sarokolaie, A. K.; Ganji, D. D. (2015): Study on blood flow containing nanoparticles through porous arteries in presence of magnetic field using analytical methods. *Physica E: Low-Dimensional Systems and Nanostructures*, vol. 70, pp. 146-156.

Hady, F. M.; Ibrahim, F. S.; Abdel-Gaied, S. M.; Eid, M. R. (2011): Boundary-layer non-Newtonian flow over vertical plate in porous medium saturated with nanofluid. *Applied Mathematics and Mechanics*, vol. 32, no. 12, pp. 1577-1586.

Hady, F. M.; Eid, M. R.; Ahmed, M. A. (2014): A nanofluid flow in a non-linear stretching surface saturated in a porous medium with yield stress effect. *Applied Mathematics and Information Sciences Letters*, vol. 2, no. 2, pp. 43-51.

Hatami, M.; Ganji, D. D. (2013): Heat transfer and flow analysis for SA-TiO2 non-Newtonian nanofluid passing through the porous media between two coaxial cylinders. *Journal of Molecular Liquids*, vol. 188, no. 2013, pp. 155-161.

Hamad, M. A. A. (2011): Analytical solution of natural convection flow of a nanofluid over a linearly stretching sheet in the presence of magnetic field. *International Communications Heat and Mass Transfer*, vol. 38, no. 4, pp. 487-492.

Khaled, S. M.; Ebaid, A.; Almutairi, F. (2014): The exact endoscopic effect on the peristaltic flow of a nanofluid. *Journal of Applied Mathematics*, vol. 2014, pp. 1-11, http://dx.doi.org/10.1155/2014/367526.

Mabood, F.; Khan, W. A.; Rashidi, M. M. (2017): The new analytical study for boundary-layer slip flow and heat transfer of nanofluid over a stretching sheet. *Thermal Science*, vol. 21, no. 1A, pp. 289-301.

Metal, T. S. Oh; Gegel, H. (1979): *Metal Forming Fundamentals and Applications, American Society of Metals*, Metals Park, OH.

Saidur, R.; Leong, K. Y.; Mohammad, H. A. (2011): A review on applications and challenges of nanofluids. *Renewable and Sustainable Energy Reviews*, vol. 15, no. 3, pp. 1646-1668.

Valinataj-Bahnemiri, P.; Ramiar, A.; Manavi, S. A.; Mozaffari, A. (2015): Heat transfer optimization of two phase modeling of nanofluid in a sinusoidal wavy channel using artificial bee colony technique. *Engineering Science and Technology*, *An International Journal*, vol. 18, no. 4, pp. 727-737.

Wang, X. Q.; Mujumdar, A. S. (2007): Heat transfer characteristics of nanofluids: a review. *International Journal of Thermal Sciences*, vol. 46, no. 1, pp. 1-19.

Wang, X. Q.; Mujumdar, A. S. (2008): A review on nanofluids-part II: experiments and applications. *Brazilian Journal of Chemical Engineering*, vol. 25, no. 4, pp. 631-648.

Xuan, Y.; Li, Q. (2003): Investigation on convective heat transfer and flow features of nanofluids. *Journal of Heat Transfer*, vol. 125, no. 1, pp. 151-155.

Yadav, D. (2017a): Electrohydrodynamic instability in a heat generating porous layer saturated by a dielectric nanofluid. *Journal of Applied Fluid Mechanics*, vol. 10, no. 3, pp. 763-776.

Yadav, D. (2017b): Numerical solution of the onset of natural convection in a rotating nanofluid layer induced by purely internal heating. *International Journal of Applied and Computational Mathematics*, vol. 3, no. 4, pp. 3663-3681.

Yadav, D.; Bhargava, R.; Agrawal, G. S. (2013): Numerical solution of a thermal instability problem in a rotating nanofluid layer. *International Journal of Heat and Mass Transfer*, vol. 63, no. 2013, pp. 313-322.

Yadav, D.; Lee, D.; Cho, H. H.; Lee, J. (2016): The onset of double-diffusive nanofluid convection in a rotating porous medium layer with thermal conductivity and viscosity variation: a revised model. *Journal of Porous Media*, vol. 19, no. 1, pp. 31-46.